Radiology: Cardiothoracic Imaging

ORIGINAL RESEARCH

Pulmonary Vascular Manifestations of COVID-19 Pneumonia

*Min Lang, MD, MSc** • *Avik Som, MD, PhD** • *Denston Carey, BS* • *Nicholas Reid, BS* • *Dexter P. Mendoza, MD* • *Efrén J. Flores, MD* • *Matthew D. Li, MD* • *Jo-Anne O. Shepard, MD* • *Brent P. Little, MD*

From the Department of Radiology, Massachusetts General Hospital, 55 Fruit St, Boston, MA 02114 (M.L., A.S., D.P.M., E.J.F., M.D.L., J.O.S., B.P.L.); and Harvard Medical School, Boston, Mass (D.C., N.R.). Received May 2, 2020; revision requested May 20; revision received June 3; accepted June 9. **Address correspondence to** B.P.L. (e-mail: *blittle@partners.org*).

*M.L. and A.S. contributed equally to this work.

Conflicts of interest are listed at the end of this article.

Radiology: Cardiothoracic Imaging 2020; 2(3):e200277 • https://doi.org/10.1148/ryct.2020200277 • Content codes: CH CT

Purpose: To investigate pulmonary vascular abnormalities at CT pulmonary angiography (CT-PE) in patients with coronavirus disease 2019 (COVID-19) pneumonia.

Materials and Methods: In this retrospective study, 48 patients with reverse-transcription polymerase chain reaction–confirmed COVID-19 infection who had undergone CT-PE between March 23 and April 6, 2020, in a large urban health care system were included. Patient demographics and clinical data were collected through the electronic medical record system. Twenty-five patients underwent dual-energy CT (DECT) as part of the standard CT-PE protocol at a subset of the hospitals. Two thoracic radiologists independently assessed all studies. Disagreement in assessment was resolved by consensus discussion with a third thoracic radiologist.

Results: Of the 48 patients, 45 patients required admission, with 18 admitted to the intensive care unit, and 13 requiring intubation. Seven patients (15%) were found to have pulmonary emboli. Dilated vessels were seen in 41 cases (85%), with 38 (78%) and 27 (55%) cases demonstrating vessel enlargement within and outside of lung opacities, respectively. Dilated distal vessels extending to the pleura and fissures were seen in 40 cases (82%) and 30 cases (61%), respectively. At DECT, mosaic perfusion pattern was observed in 24 cases (96%), regional hyperemia overlapping with areas of pulmonary opacities or immediately surrounding the opacities were seen in 13 cases (52%), opacities associated with corresponding oligemia were seen in 24 cases (96%), and hyperemic halo was seen in 9 cases (36%).

Conclusion: Pulmonary vascular abnormalities such as vessel enlargement and regional mosaic perfusion patterns are common in COVID-19 pneumonia. Perfusion abnormalities are also frequently observed at DECT in COVID-19 pneumonia and may suggest an underlying vascular process.

Supplemental material is available for this article.

Since December 2019, infection by novel coronavirus severe acute respiratory syndrome coronavirus 2 has erupted into a global pandemic, with more than 2.3 million reported cases worldwide to date (1). The parenchymal imaging findings of coronavirus disease 2019 (COVID-19) pneumonia have been well described, including multifocal peripheral ground-glass opacities with or without consolidation (2–5). However, these findings are not specific and can be seen in various other diseases, including other viral pneumonias, atypical bacterial pneumonia, drug toxicity, eosinophilic pneumonia, or cryptogenic organizing pneumonia (3,6–8).

Progression to acute respiratory distress syndrome (ARDS) has been reported in 20% of COVID-19 pneumonia cases and in up to 41% of patients who are hospitalized (9). However, some patients requiring intubation have relatively preserved lung compliance, suggesting involvement of other processes in addition to parenchymal damage. Recent studies have proposed that loss of perfusion regulation and loss of normal physiologic hypoxic vasoconstriction contribute to the hypoxemia seen in patients with COVID-19 (10,11). In addition, there has been increasing concern for hypercoagulability and pulmonary embolism (PE) in patients with COVID-19, with a few concordant autopsy studies reporting findings of pulmonary microthrombi (12–17). Finally, regional and diffuse pulmonary vascular pathology has also been suggested, including conditions mimicking high-altitude pulmonary edema (18). Consistent with vascular pathology playing an important role in the pathophysiology of COVID-19 pneumonia, prior reports did note a high prevalence of vessel enlargement and thickening within areas of pulmonary parenchymal opacity in patients with COVID-19 (2,4,5). However, to our knowledge, a detailed investigation of pulmonary vascular findings at CT is lacking in the literature.

Recently, we observed perfusion abnormalities in several patients with COVID-19 infection who underwent dual energy CT (DECT) imaging for suspicion of PE (19). These perfusion changes further support an underlying vascular pathology, but systematic investigation of its manifestation in COVID-19 pneumonia has not been described. Our goal was to assess

Abbreviations

ACR = American College of Radiology, ARDS = acute respiratory distress syndrome, COVID-19 = coronavirus disease 2019, CT-PE = CT pulmonary angiography, DECT = dual-energy CT, IQR = interquartile range, PE = pulmonary embolism, RSNA = Radiological Society of North America, RT-PCR = reverse-transcription polymerase chain reaction, STR = Society of Thoracic Radiology

Summary

Pulmonary vessels and perfusion are frequently abnormal in coronavirus disease 2019 (COVID-19) pneumonia and may point to a key role of pulmonary vascular pathology and hypoxemia in COVID-19.

Key Points

- Medium-to-small vessel dilatation is highly prevalent in coronavirus disease 2019 (COVID-19) pneumonia, is not confined to areas of diseased lung, and often involves subpleural vessels, suggesting a diffuse vascular process.
- Perfusion abnormalities are common features of COVID-19 pneumonia, including mosaic perfusion, focal hyperemia in a subset of pulmonary opacities, focal oligemia associated with a subset of peripheral opacities, and rim of increased perfusion around an area of low perfusion ("hyperemic halo" sign).
- Dual-energy CT pulmonary angiography provides insight on the vascular manifestations of COVID-19 pneumonia.

pulmonary vascular findings at CT, including the prevalence of PE in our cohort, abnormalities of pulmonary vessels, and mosaic attenuation. In addition, we used DECT, available on a subset of our scanners, to obtain pulmonary blood volume images and assess lung perfusion patterns in COVID-19 pneumonia.

Materials and Methods

Study Design and Setting

This retrospective study was performed at the Partners Healthcare system, a large, quaternary academic medical center. This study was approved by the institutional review board with a waiver of informed consent, and patient privacy was ensured in compliance with the Health Care Information Portability and Accountability Act. All procedures and practices were in accordance with the Declaration of Helsinki.

Study Cohort

Between March 23 and April 6, 2020, 353 CT pulmonary angiography (CT-PE) studies were completed across the Partners Healthcare system for patients in an inpatient or emergency department setting. Of these patients, 51 had a positive reverse-transcription polymerase chain reaction (RT-PCR) analysis for COVID-19 infection via nasopharyngeal swab at any point during their stay in the hospital or emergency department and were included in this retrospective study. The time range between the RT-PCR test and CT-PE study was 0 to 14 days, with RT-PCR always performed on the same day or preceding the CT-PE study. Three patients with nondiagnostic CT-PE studies were excluded from the study due to excessive motion. The remaining 48 patients were included in this study.

Table 1: Summary of Patient Characteristics

Characteristic	Patients (*n* = 48)
Mean age ± SD (y)	58 ± 19
Sex	
Male	25 (52)
Female	23 (48)
Ethnicity	
White	26 (54)
African American	6 (13)
Hispanic	12 (25)
Other	4 (8)
Presenting symptoms	
Fever	29 (60)
Chills	12 (25)
Myalgia	14 (29)
Cough	34 (71)
Shortness of breath	28 (58)
Chest pain	12 (25)
Anosmia	4 (8)
Hemoptysis	1 (2)
GI symptoms	13 (27)
Fatigue	17 (35)
Cognitive change	5 (10)
Comorbidities	
Current smoker	0 (0)
Ex-smoker	12 (25)
Hypertension	23 (48)
Diabetes	9 (19)
Obesity	21 (44)
Heart failure	5 (10)
COPD	2 (4)
History of malignancy	11 (23)
History of DVT or PE	6 (13)
Recent surgery	1 (2)
Oxygenation requirement	
Nasal cannula	35 (73)
Intubation	13 (27)
Current clinical status	
Admitted	45 (94)
ICU	18 (38)
Discharged	14 (29)
Deceased	2 (4)

Note.—Unless otherwise noted, data are numbers of patients, with percentages in parentheses. COPD = chronic obstructive pulmonary disease, DVT = deep venous thrombosis, GI = gastrointestinal, ICU = intensive care unit, PE = pulmonary embolus, SD = standard deviation.

Patient demographics, date of admission, comorbidities, clinical course, and laboratory findings were retrospectively collected through our electronic medical record system.

Table 2: Pulmonary Opacities at Chest CT

Finding	Patients (n = 48)
Opacities	
Ground glass	44 (92)
Consolidation	35 (73)
Distribution	
Central	5 (11)
Peripheral	27 (61)
Diffuse	12 (27)
Lobar severity score (range: 0–3)	
Right upper	1.6
Right middle	1.3
Right lower	2
Left upper	1.7
Left lower	1.9
Averaged total lung severity score (range: 0–15)	8.3 ± 4.6*
RSNA/STR/ACR category	
Typical	27 (56)
Indeterminate	11 (23)
Atypical	6 (13)
Negative for pneumonia	4 (8)

Note.—Unless otherwise noted, data are numbers of patients, with percentages in parentheses. ACR = American College of Radiology, RSNA = Radiological Society of North America, STR = Society of Thoracic Radiology.
*Mean ± standard deviation.

CT Image Acquisition

All images were obtained with patient in the supine position using one of the following CT systems: Discovery CT750 HD (GE Healthcare, Milwaukee, Wis), Revolution Frontier (GE Healthcare), SOMATOM Definition Flash (Siemens Healthineers, Erlangen, Germany), SOMATOM Definition AS (Siemens Healthineers), SOMATOM Force (Siemens Healthineers), and Aquilion ONE (Toshiba, Tokyo, Japan). The main scanning parameters were: tube voltage, 140 kVp (plus 80 kVP for dual energy); matrix, 512 × 512; slice thickness, 1.25 mm; field of view, 440 mm × 440 mm. CT imaging was not used for screening or primary diagnosis of COVID-19 at our institution but was used to assess potential complications or help guide clinical management in difficult cases.

Lung Parenchymal Findings

CT-PE images for all patients were retrospectively and independently analyzed by two thoracic radiologists (B.P.L. and D.P.M., 11 years and 2 years of thoracic imaging subspecialty experience) using standard picture archiving and communication system viewing software and standard viewing windows. Disagreement in CT scoring and categorization of CT patterns was resolved by consensus discussion with a third thoracic radiologist (E.J.F., 7 years of subspecialty experience). All radiologists were blinded to the original radiology report and to clinical and laboratory findings.

All studies were evaluated for presence of ground-glass or consolidative opacities, predominant distribution of opacities (peripheral–distal 1/3 of the lung, central–central 2/3 of the lung, or diffuse). Each lobe was also graded quantitatively on a severity score for opacities ranging from 0 to 4 (0 = none, 1 = 1%–25%, 2 = 26%–50%, 3 = 51%–75%, 4 = 76%–100%), and a total severity score was calculated by summing the scores of all 5 lobes.

The images were categorized on the basis of the Radiological Society of North America (RSNA)/Society of Thoracic Radiology (STR)/American College of Radiology (ACR) reporting guidelines, as either having "no evidence of pneumonia," an "atypical appearance," an "indeterminate appearance," or a "typical appearance" for COVID-19 pneumonia (20). Briefly, these guidelines note that a "typical appearance" is characterized by having any of the following, including peripheral bilateral ground-glass opacities with or without consolidation or intralobular lines, multifocal ground-glass opacity with rounded morphology with or without consolidation, or a reverse halo sign. "Indeterminate findings" were defined as having the absence of typical features, and any of the following features, including: presence of ground-glass opacities with or without consolidation in a nonrounded morphology that can be in a nonperipheral, perihilar, or diffuse distribution. In addition, cases with a few small ground-glass opacities with a nonrounded morphology and nonperipheral distribution constituted indeterminate findings per the RSNA reporting guidelines. Further, an atypical appearance was defined as the absence of typical or indeterminate features, with presence of either lobar or segmental consolidation without ground-glass opacities. Additional findings, including discrete centrilobular nodules, lung cavitation, or smooth interlobular septal thickening with pleural effusion, were also categorized as features of atypical appearance. If there were no CT findings to suggest pneumonia, the CT scan was assigned the category of "negative for pneumonia."

CT-PE Study Findings

All CT-PE images were evaluated for presence of PE and pulmonary infarct (such as wedge-shaped ground-glass opacities), main pulmonary artery diameter, and evidence of right heart strain (right ventricle–to–left ventricle short axis > 1) (21). Additional parameters recorded at CT lung window (−500 to 1000 Hounsfield units) include presence of reverse halo sign, presence of septal thickening, emphysema, centrilobular nodules, or bronchial wall thickening. In addition, radiologists evaluated the pulmonary vasculature specifically for the following signs: vessel enlargement within areas of parenchymal opacity, vessel enlargement outside of opacities, dilated distal subsegmental vessels touching pleura or fissures, and mosaic attenuation pattern (areas of more lucent/oligemic lung adjacent

to areas of diseased lung) in areas of the lung outside of the pulmonary opacities. Vessel enlargement was defined as vessel diameter larger than expected for the point within the vascular tree, characterized by: *(a)* vessel diameter larger than that in adjacent portions of nondiseased lung, *(b)* vessel diameter larger than that in comparable regions of nondiseased contralateral lung, or *(c)* focal dilatation or nontapering of vessels as they course toward the lung periphery.

DECT Technique and Findings

DECT was performed on 25 patients. These images were qualitatively assessed for mosaic perfusion (areas of heterogeneity on the pulmonary blood volume images with alternating relatively higher and lower perfusion), focal hyperemia (areas of relative increase in perfusion compared with background lung), focal oligemia (areas of relative decrease in perfusion compared with background lung), and presence or absence of a rim of increased perfusion around an area of low perfusion (compared with background lung) corresponding to a parenchymal opacity–a "hyperemic halo" sign.

Statistical Analysis

Normally distributed data were presented as mean ± standard deviation, nonnormally distributed data as median (interquartile range [IQR]), and categorical variables as frequency (%). CIs of proportions were calculated. Spearman ρ correlation coefficients were used for correlation between variables, and κ interrater variable was used for statistical analysis of normally distributed data presented as mean ± standard deviation, nonnormally distributed data as median (IQR), and categorical variables as frequency (%). Spearman rank correlation was used to evaluate nonparametric, nonlinear data, and Pearson correlation was used to evaluate continuous normally distributed data. *P* value less than .05 was considered statistically significant. Statistical analysis was performed using Prism (Graphpad, San Diego, Calif), RStudio (RStudio, Boston, Mass), and Stata (Stata, College Station, Tex).

Table 3: Vascular and Perfusion Findings

Finding	Patients
Pulmonary angiogram finding (*n* = 48)	
Positive for pulmonary emboli	7 (15)
Multilobar	6 (13)
Pulmonary infarcts	3 (6)
Right heart strain	1 (2)
Number of patients in the ICU	2 (4)
No. of patients intubated or deceased	0 (0)
No. of patients with risk factors	4 (8)
History of arrhythmia	2 (4)
History of malignancy	4 (8)
History of PE or DVT	2 (4)
Recent surgery	0 (0)
D-dimer (ng/mL)	
Positive for PE	6136 ± 3951
Negative for PE	3653 ± 1439
Dilated main pulmonary artery	8 (17)
Vessel enlargement	41 (85)
Within opacity	38 (79)
Outside of opacity	27 (56)
Extension to pleura	40 (83)
Along fissures	30 (63)
Mosaic perfusion pattern	45 (94)
Dual-energy CT finding (*n* = 25)	
Mosaic perfusion	24 (96)
Mild	1 (4)
Moderate	17 (68)
Severe	6 (24)
Regional hyperemia	13 (52)
Regional oligemia	24 (96)
Hyperemic halo	9 (36)

Note.—Unless otherwise noted, data are numbers of patients, with percentages in parentheses. DVT = deep venous thrombosis, ICU = intensive care unit, PE = pulmonary embolus.

Results

A total of 48 patients were included in this retrospective study. The average age was 58 years ± 19, and 23 patients (48%) were women (Table 1). The most common manifesting symptoms included cough (71%), fever (60%), and shortness of breath (58%). Hypertension (48%), obesity (44%), history of malignancy (23%), and diabetes (19%) were the four most prevalent comorbidities. No patients had prior liver disease. Only two (4%) patients had a pre-existing pulmonary condition of chronic obstructive pulmonary disease. Six (13%) patients had a history of PE. Forty-five patients (94%) required admission, with 18 patients (38%) requiring admission to the intensive care unit. Thirty-five patients (73%) required nasal cannula to maintain oxygen saturation above 90% during admission, with 13 (27%) of these patients eventually requiring intubation. At the date of last follow-up, 14 patients were discharged (29%), and two patients who required intubation were deceased (4%).

Consistent with previous reports, the most common features seen at chest CT of patients with COVID-19 are multilobar ground-glass opacities with or without consolidation in a predominantly peripheral distribution (Table 2); of note, the distribution was assessed in 44 cases, as four studies were categorized as negative for pneumonia without evidence of opacity. The average severity scores of individual lobes are listed in Table 2 and were significantly different between the lobes (*P* = .03), with both lower lobes having a higher average severity score (average left lower lobe severity score of 1.9 of 3, and average right lower lobe severity score 2 of 3) than the other lobes (range 1.3–1.7 of 3) (Table 2). On the basis of the RSNA/STR/ACR consensus guidelines, the findings were classified as typical in 56% of cases,

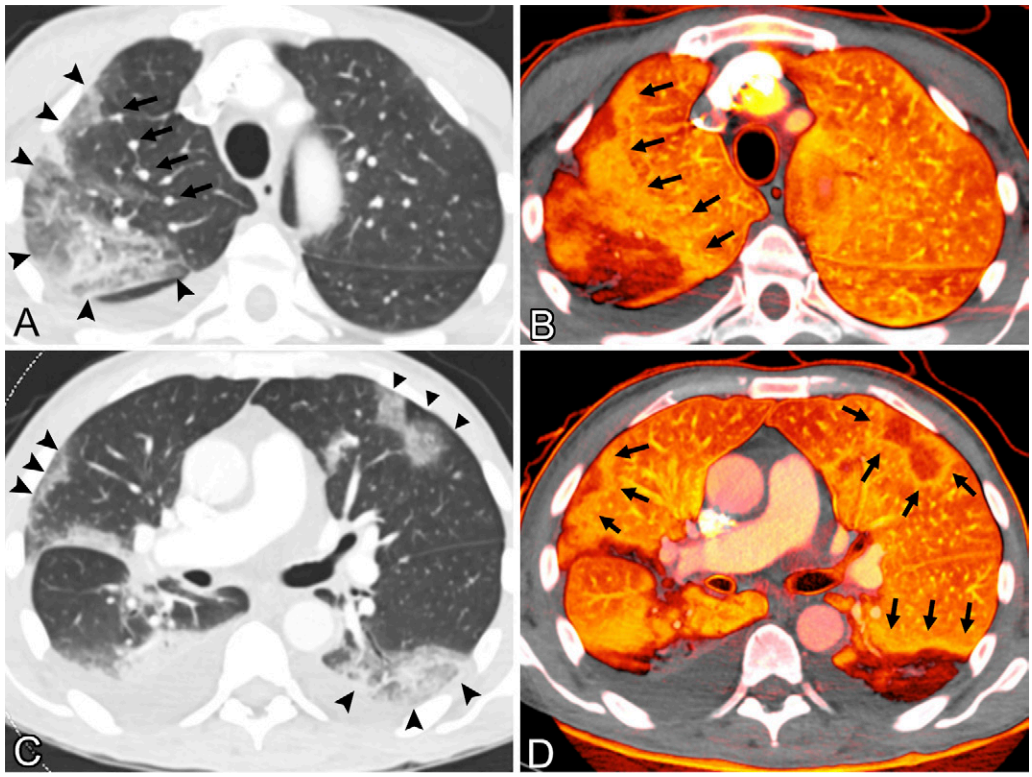

Figure 1: Images in a 69-year-old man hospitalized for fever, weakness, and chills, found to have coronavirus disease 2019. CT pulmonary angiogram was obtained on day 4 of admission for acute intermittent tachycardia, desaturation, and new complaint of shortness of breath. The study was negative for pulmonary emboli. *A*, Contrast-enhanced CT pulmonary angiogram of the upper lungs at lung windows shows a region of peripheral ground-glass opacity and consolidation in the right upper lobe (arrowheads); the subsegmental vessels within the opacities are dilated, and the right upper lobe vessels proximal to the opacity are also dilated (arrows). *B*, Pulmonary blood volume (PBV) image at the same level shows a large peripheral perfusion defect corresponding to the distribution of right upper lobe opacity, with a surrounding halo of increased perfusion (arrows). There is also heterogeneous perfusion of the left upper lobe. *C*, CT image of the lower lungs in the same patient shows peripheral ground-glass opacities and consolidation in the lower lobes, middle lobe, and lingula with a somewhat round or wedge-shaped appearance (arrowheads). *D*, PBV image shows perfusion defects corresponding to the areas of opacity in *C*, with surrounding halos of increased perfusion (arrows).

indeterminate in 23%, atypical in 13%, and negative for pneumonia in 8% (Table 2).

A total of seven patients (15%) were found to have PE (Fig E1 [supplement]), with six cases (13%) involving arteries of multiple lobes, three cases (6%) exhibiting pulmonary infarcts, and one case (2%) with evidence of right heart strain (Table 3) (22). Two of the seven patients with PE were admitted to the intensive care unit and did not require intubation. Main pulmonary artery dilatation (23) (≥ 30 mm) was observed in eight patients (17%) (24). Patients with PE had on average significantly higher D-dimer levels than patients without PE (6136 ng/mL ± 3951 vs 3653 ng/mL ± 1439, respectively; $P = .02$) (Table 3).

Overall, dilated pulmonary vasculature was seen in 41 (85%) cases, with 38 (79%) within pulmonary opacities and 27 (56%) outside of the opacities (Table 3; Figs 1, *A*, 2, 3, *C*), and dilated distal pulmonary vessels extending to the pleura and fissures were seen in 40 cases (83%) and 30 cases (63%), respectively (Figs 4 *A* and *B*, 5). As described, vascular enlargement was often within or outside the opacity and extended to the pleura generally near ground-glass opacities without diffuse involvement. Ten of our patients had chest CT imaging available that was performed within 6 months prior to COVID-19 infection, and none of the vascular findings or evidence of pulmonary hypertension were observed previously. Mosaic attenuation, likely from mosaic perfusion, was noted in 45 cases (94%) at conventional chest CT lung window (−500 to 1000 Hounsfield units). Dilated pulmonary vessels even outside of vessels with emboli were seen in five of seven patients with PE.

Overall, DECT was performed in 25 cases (52%). A mosaic perfusion pattern was observed in 24 cases (96%), with one (4%) categorized as mild, 17 (68%) as moderate, and six (24%) as severe (Table 3; Figs 1, *B* and *D*, 2, *B* and *D*, 3, *B* and *D*). More specifically, regionally increased hyperemia overlapping with areas of pulmonary opacities or immediately surrounding the opacities were seen in 13 cases (52%). Pulmonary opacities associated with corresponding oligemia at DECT were observed in 24 cases (96%). Intensely hyperemic area surrounding oligemic pulmonary opacities forming a peripheral hyperemic halo was noted in nine cases (36%). Of note, all seven patients with PE exhibited perfusion abnormalities at DECT: Seven had mosaic perfusion, four had hyperemia overlapping with areas of pulmonary opacities, seven had oligemia, and four had hyperemic halo. Figure E2 (supplement) provides a reference of normal conventional chest CT and DECT images in a patient with COVID-19 infection but without respiratory symptoms and without lung parenchymal abnormalities

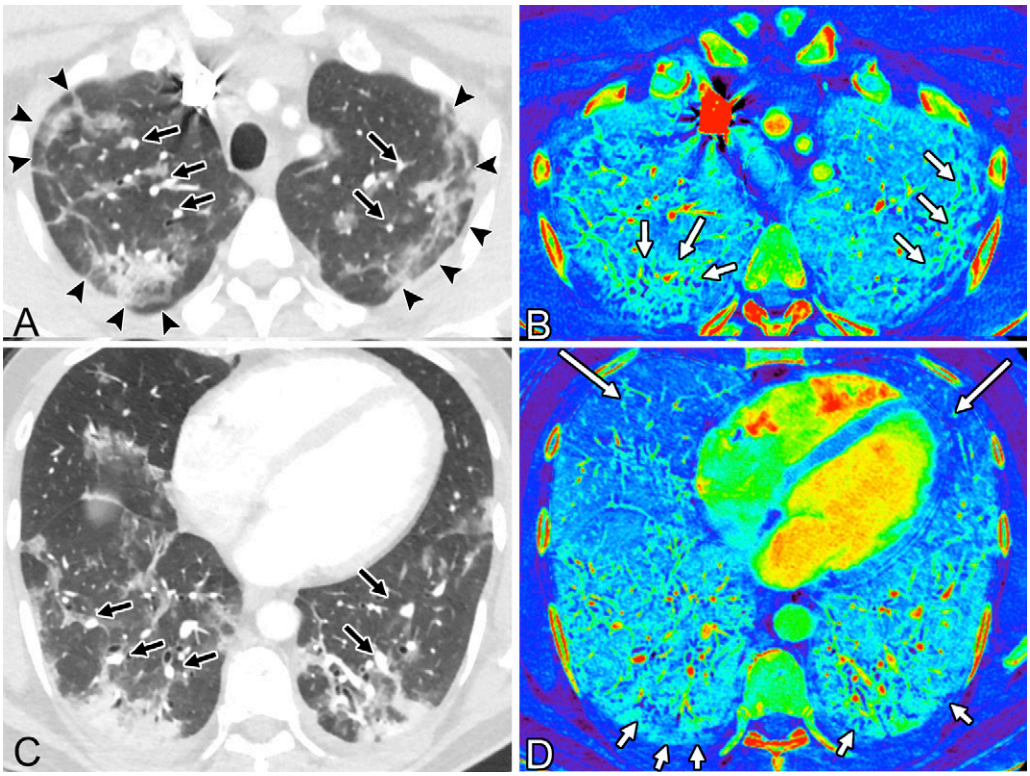

Figure 2: Images in a 45-year-old man who presented with cough and fever, requiring supplemental oxygen via nasal cannula, and was found to have coronavirus disease 2019. On day 5 of admission, patient underwent CT pulmonary angiography for acute shortness of breath, tachypnea, and an elevated D-dimer level. *A*, Contrast-enhanced CT pulmonary angiogram of the upper lungs shows multiple ground-glass opacities and consolidation with a peripheral predominance; several perilobular bands of consolidation suggest an organizing lung injury pattern (arrowheads). Subsegmental vessels supplying regions of opacity are dilated (arrows). *B*, Corresponding iodine map image shows increased perfusion of some areas of opacity (arrows). *C*, Axial CT image as part of the same examination shows additional peripheral ground-glass opacities and consolidation in the lower lungs, with enlarged vessels within and supplying regions of lung with opacity (arrows), while vessels in the anterior lungs are smaller in caliber with relatively lower regional attenuation of the anterior lungs. *D*, Corresponding iodine map image shows increased perfusion to the posterior lower lobes in general, decreased perfusion of the anterior lungs (long arrows), and small perfusion defects corresponding to posterior areas of opacity seen in *C* (short arrows).

at imaging; CT pulmonary angiogram was obtained for chest pain, tachycardia, and elevated D-dimer. Finally, of the 25 patients who underwent DECT, perfusion abnormalities were seen in all patients who required intubation or were deceased (four of four patients) and in 95% of patients who did not require intubation (20 of 21 patients).

Discussion

The pulmonary response to pneumonia is generally characterized by hypoxic pulmonary vasoconstriction and reduced perfusion to the sites of parenchymal disease, resulting in shunting of blood away from most affected and toward less affected regions–a beneficial matching of ventilation and perfusion (25). Our finding of frequent and pronounced dilatation of vasculature to regions of diseased lung may be suggestive of disordered vasoregulation, leading to substantial ventilation and perfusion mismatch even early in the disease. This finding may explain in part the hypoxemia that can occur in COVID-19 pneumonia despite normal pulmonary compliance (10,11). Although attention has been previously given to the role of endothelial damage and resulting dysregulation of hypoxic vasoconstriction in the setting of ARDS (26), we hypothesize that abnormal pulmonary vasoregulation may play a large role in patients with COVID-19 infection even before the presence of radiologic or clinical features that would suggest ARDS and may be even more pronounced when ARDS does occur.

In normal lung, distal subsegmental vessels are usually inconspicuous within the subpleural regions. A substantial number of patients in our study, however, exhibited dilated and sometimes tortuous distal vessels in the subpleural lung. This phenomenon is distinct from the pulmonary vascular thickening (or the "thick vessel sign") within pulmonary opacities in COVID-19 pneumonia that has been reported to range from 59% to 82% in patients with COVID-19 (2,4,5). This finding is nonspecific and can be seen in conditions such as pulmonary hypertension, pulmonary venous hypertension, pulmonary veno-occlusive disease, hepatopulmonary syndrome, and portopulmonary hypertension (27). However, patients in this study with imaging prior to COVID-19 infection had none of these findings, which argues against a chronic process. Moreover, there was a lack of hepatic disease or other pre-existing pulmonary conditions that would provide a reason for the vascular pathology.

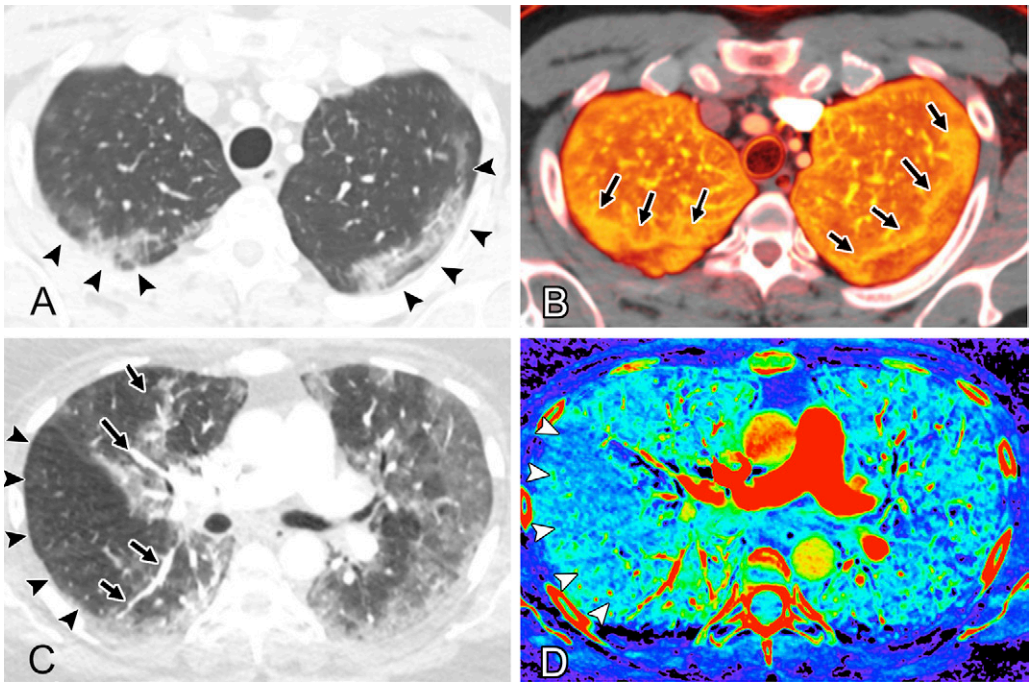

Figure 3: *A, B,* Images in a 41-year-old man who presented to the emergency department with acute shortness of breath and underwent CT pulmonary angiography for concern for pulmonary embolism. Patient tested positive for coronavirus disease 2019 infection. *A,* Peripheral ground-glass opacities are present in the posterior upper lobes (arrowheads); regional dilatation of vessels is noted in adjacent upper lobes. *B,* Pulmonary blood volume image at the same level shows peripheral perfusion defects corresponding to the opacities, with surrounding halos of increased perfusion (arrows). *C, D,* Images in a 57-year-old woman who presented with 7 days of fever, malaise, chills, cough, and increasing shortness of breath. On day 3 of admission, patient developed increasing oxygen requirement and elevated D-dimer level. *C,* CT scan of the upper lungs at lung windows shows ground-glass opacities in the central and peripheral upper lungs bilaterally, with regional low attenuation of a portion of the right upper lobe and superior segment of the right lower lobe (arrowheads). Vessels within the low attenuation region are diminutive in a regional pattern, while vessels in the areas of ground-glass opacity are dilated (arrows). *D,* Corresponding iodine map image shows regional decreased perfusion to the right lung (white arrowheads) and increased perfusion to the areas of ground-glass opacity, while there is also heterogeneous perfusion of the left upper lobe.

Diffuse alveolar damage is a hallmark of ARDS and can be caused by noninfectious etiologies and infectious etiologies, including viral pneumonia such as severe acute respiratory syndrome, Middle East respiratory syndrome, and influenza (28–32). Development of ARDS-related thrombosis was thought to be the result of fibrin deposition due to endothelial injury (33). A recent autopsy study on a series of patients with COVID-19 infection, however, reported not only findings of widespread macro- and microthrombosis, but also angiopathy and notably increased angiogenesis (34). Furthermore, in this recent report, fibrin thrombi were seen in all patients with COVID-19 infection, and angiogenesis was observed 2.7 times higher in patients with COVID-19 infection than those with influenza. While this provides additional validation of prior autopsy reports describing microthombosis and small vessel thickening in patients with COVID-19 pneumonia, it also provides evidence of more widespread vascular pathologies, such as angiogenesis and endothelial inflammation. These vascular mechanisms also appear to play a larger role in COVID-19 pneumonia than other viral pneumonias such as influenza (34). The vascular abnormalities we observed at CT imaging correlate well with these pathology findings and support the notion of diffuse vascular abnormalities in COVID-19 pneumonia. The underlying mechanisms of these findings, however, may be related to vascular inflammation, endothelial damage, microthrombosis, dysfunctional vasoregulation, or a combination thereof (10,30,34–38). Further radiologic-pathologic correlation investigations are needed to better elucidate the underlying vascular phenomenon.

DECT is a powerful imaging tool used to characterize pulmonary blood volume and patterns of pulmonary perfusion by taking advantage of the different attenuation profiles of different substances (39,40). This is achieved by utilizing two different x-ray energy spectra concurrently during imaging. DECT is part of the standard PE CT protocol at a subset of hospitals within our health care system. In the COVID-19 setting, DECT may provide insight into the physiologic process of vascular shunting. Of the 25 patients who underwent DECT in our study, mosaic perfusion abnormalities were seen in 24 patients (96%), with predominately increased perfusion proximal to areas of lung opacities. Mosaic perfusion is a subset of mosaic attenuation and can be broadly categorized into two etiologic categories: small airway disease with hypoxemic vasoconstriction due to air trapping, or small vessel disease (40,41). While mosaic attenuation and perfusion can be seen in infections because of diffuse airway abnormalities and/or mucus plugging, the perfusion changes in our patients did not correlate in most cases with bronchial wall thickening, visible secretions, mucous plugging, or emphysema, arguing against small airway disease as a sole or primary

underlying cause. Furthermore, the perfusion abnormalities had a regional rather than lobular distribution and extended beyond areas of parenchymal lung opacity, suggesting the possibility of a diffuse vascular process.

There were decreased areas of peripheral perfusion corresponding to peripheral lung opacities in 24 of 25 patients who underwent DECT (96%). This radiographic observation can be consistent with ARDS, as areas of oligemia can be seen in ARDS-related thrombosis (33). The opacities with corresponding decreased perfusion may represent filling of airspaces and interstitium with exudates, or possibly peripheral areas of infarction mediated by small vessel thrombosis. Furthermore, of the 25 patients who underwent DECT, perfusion abnormalities were observed in all patients who required intubation or were deceased and in 95% of patients who did not require intubation. This suggests that perfusion abnormalities are highly prevalent in symptomatic patients who required admission. The small number of patients who underwent DECT, however, limited meaningful correlation of these findings to degree of hypoxemia or clinical outcome, which will require further investigation. Interestingly, however, there was a peripheral halo of increased perfusion surrounding peripheral opacities in nine patients (36%). This appearance is not typical in ARDS or acute or chronic PE, in which uniformly decreased perfusion is seen within affected areas. The peripheral halo of increased perfusion observed in our study has neither been described in the literature nor noted in our practice in cases of pulmonary infarction due to bland PE but has been described once previously in a case of bacterial pneumonia (40). This suggests an interplay between inflammatory processes and vascular phenomena in a subset of COVID-19 pneumonia. Further research into whether DECT may provide prognostic information for patients with COVID-19 is needed.

There are multiple possible causes of differential pulmonary perfusion. PE, pulmonary hypertension, and vasculitis are additional conditions that can alter pulmonary perfusion (42). PE and pulmonary hypertension as the primary underlying causes of mosaic perfusion in our cohort of patients with COVID-19 pneumonia are unlikely given that perfusion abnormalities were seen in patients without visible PE and often did not correspond to areas supplied by the pulmonary arteries containing thrombus; furthermore, our patients did not have a history of pulmonary hypertension, and only a small proportion of patients exhibited a mildly dilated main pulmonary artery (17%). Vasculitis secondary to infection can have varying appearances at imaging, including vessel wall thickening, cavitary lesions, and ground-glass or consolidative opacities (43). However, it would be unusual for isolated involvement of medium-to-small pulmonary vessels, and there is a lack of concordant findings reported on pathology (13,16).

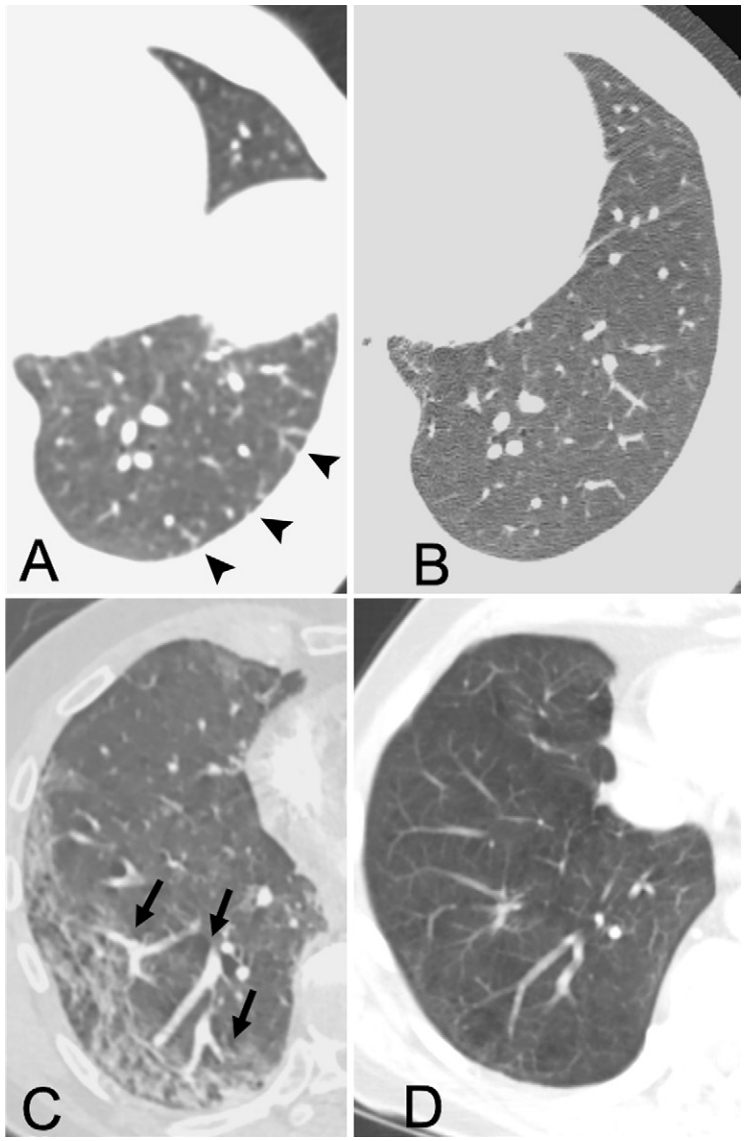

Figure 4: *A, B,* Images in a 47-year-old woman with a history of metastatic breast cancer who initially presented with nausea, vomiting, and low-grade fever and tested positive for coronavirus disease 2019 (COVID-19) infection. Patient underwent CT pulmonary angiography (CT-PE) on day 4 of admission for acute intermittent tachycardia, lethargy, and new oxygen requirement. *A,* Axial CT image with lung windows through the left lower lobe at time of presentation shows abnormally dilated distal subsegmental vessels in the subpleural lung touching the pleural surface (arrowheads). *B,* Image at the same level of CT in the same patient 11 days prior shows normal vessel sizes and appearances, with a normal appearance of the subpleural lung. *C, D,* Images in a 64-year-old man who presented with acute onset of fatigue, headache, cough, fever, and shortness of breath and tested positive for COVID-19. On day 12 of admission, patient developed increasing oxygen requirement and CT-PE was performed. *C,* Axial CT image with lung windows through the right lower lung shows peripheral regional ground-glass opacity in the right lower lobe, with dilated segmental and subsegmental vessels supplying the region of opacified lung (arrows) and smaller diameters of vessels in unaffected lung. *D,* Image at the same level of a CT scan in the same patient approximately 3 months prior shows normal appearance of vessels.

There has been suggestion that the pathophysiology underlying COVID-19 pneumonia may resemble high-altitude pulmonary edema (18). While there are imaging similarities, including patchy ground-glass opacities, dilated vasculature, and regional perfusion changes (44–46), the fundamental mechanism may be different, as COVID-19 is likely inflammation mediated,

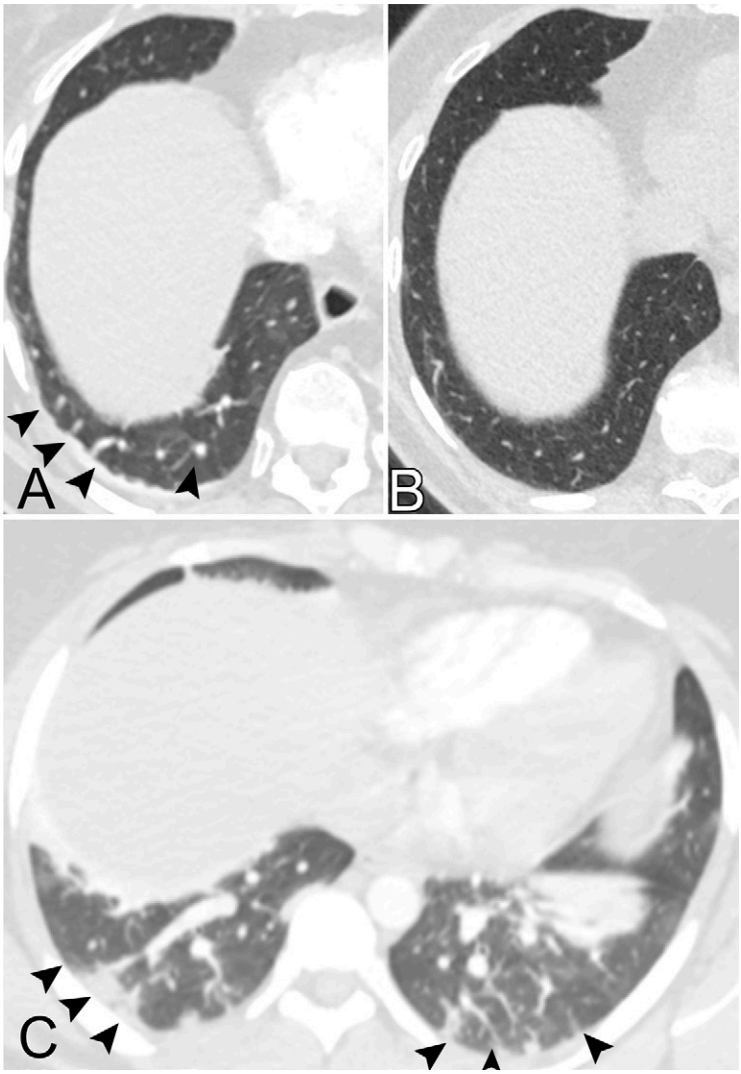

Figure 5: *A*, Image in an 84-year-old woman with a history of breast cancer who presented to the emergency department for fever, weakness, altered mental status, acute shortness of breath, and chest pain, for which CT pulmonary angiogram was obtained. Axial CT image shows dilated, nontapering, tortuous vessels in the posterior right lower lobe (arrowheads), some of which extend to the pleural surface. *B*, CT scan in the same patient shown at the same level 5 months prior shows normal vessels. *C*, Image in a 27-year-old woman who presented to the emergency department with acute shortness of breath and dyspnea on exertion. Patient was subsequently found to be coronavirus disease 2019–positive and had worsening tachypnea. Axial CT image through the lower lobes shows multiple dilated tortuous vessels within the lower lobes, with extension to the pleural surfaces (arrowheads).

whereas high-altitude pulmonary edema is characterized by uneven pulmonary vasoconstriction, increased pulmonary artery pressure, and endothelial leakage (47). Abnormal inflammation-mediated vasodilatory response in COVID-19 pneumonia may result in intrapulmonary shunting toward areas of impaired gas exchange and worsening of ventilation-perfusion mismatch, possibly explaining the enlarged vessels leading to and within areas of parenchymal opacity seen in our study.

The theory that patients with COVID-19 are at higher risk of both venous and arterial thrombosis has also recently garnered attention. The reported risk of venous thromboembolism in patients with COVID-19 has been reported to range from 25% to 31% (12,14). The incidence of PE specifically has been reported to range from 14% to 30% (12,15,48–50). Similarly, seven patients (15%) in our study were found to have PE, four of whom had risk factors including history of arrhythmia, malignancy, or prior PE or deep vein thrombosis. Acute PE, therefore, may be a potential concern in patients with COVID-19, similar to other viral pneumonias and critically ill patients in general (51–53). In addition to medium-to-large vessel thrombosis, a handful of autopsy reports of COVID-19 have reported findings of microthrombosis and small vessel thickening, which can be seen in the setting of ARDS, coagulopathies, and other etiologies of vessel injury (13,16,54).

Our study had several limitations. The study was retrospective, and the patient cohort size was relatively small given our inclusion criteria of COVID-19 patients who underwent CT-PE during a 2-week window. Most patients in the study did not have a recent prior chest CT that would allow us to assess the temporal development of imaging findings, and it is possible that some of the vascular abnormalities predated the CT scans obtained during the acute illness. Many of the findings we detected were nonspecific and can occur in other diseases, and our study was not designed to assess the specificity of the findings for COVID-19 pneumonia. DECT images were only available for 25 patients due to availability of scanners at different hospitals across our health care system, and inspiratory and expiratory phases were not performed as part of the standard imaging protocol, which may potentially confound mosaic patterns seen on CT images. Our study was also limited by the lack of control groups: patients without COVID-19 infection or those with COVID-19 infection but who did not require admission. Future studies with matched control groups, as well as patients with other appropriate pathologies, including organizing pneumonia and influenza, would be helpful to further clarify the extent of these vascular findings. Finally, assessment of vessel enlargement and mosaic perfusion can be subjective and therefore requires further confirmation with larger multireader studies or quantitative methods of categorization.

In conclusion, COVID-19 pneumonia appears to be associated with pulmonary vascular and pulmonary perfusion derangements that are caused by unclear mechanisms. Pulmonary vessel dilatation occurs not only within lung opacities, but also occurs in a regional pattern outside of parenchymal opacities and sometimes involves the subpleural lung. Perfusion abnormalities are also frequently seen at DECT imaging. Further imaging and pathologic studies are required to investigate the possible contributions of abnormal vasoregulation, intrapulmonary shunting, and/or microvascular thrombosis.

Author contributions: Guarantor of integrity of entire study, B.P.L.; study concepts/study design or data acquisition or data analysis/interpretation, all authors; manuscript drafting or manuscript revision for important intellectual content, all authors; approval of final version of submitted manuscript, all authors; agrees to ensure any questions related to the work are appropriately resolved, all authors; literature research, M.L., A.S., D.C., N.R., D.P.M., B.P.L.; clinical studies, M.L.,

A.S., D.C., N.R., D.P.M., E.J.F., B.P.L.; statistical analysis, M.L., A.S., D.C., E.J.F.; and manuscript editing, all authors

Disclosures of Conflicts of Interest: **M.L.** disclosed no relevant relationships. **A.S.** disclosed no relevant relationships. **D.C.** disclosed no relevant relationships. **N.R.** disclosed no relevant relationships. **D.P.M.** disclosed no relevant relationships. **E.J.F.** Activities related to the present article: disclosed no relevant relationships. Activities not related to the present article: disclosed grant funding paid to author from the American College of Radiology Innovation Fund and the National Cancer Institute Research Diversity Supplement for work not related to this manuscript. Other relationships: disclosed no relevant relationships. **M.D.L.** disclosed no relevant relationships. **J.O.S.** disclosed no relevant relationships. **B.P.L.** Activities related to the present article: disclosed no relevant relationships. Activities not related to the present article: disclosed money paid to author from Elsevier for textbook author and editor royalties. Other relationships: disclosed no relevant relationships.

References

1. Huang C, Wang Y, Li X, et al. Clinical features of patients infected with 2019 novel coronavirus in Wuhan, China. Lancet 2020;395(10223):497–506 [Published correction appears in Lancet 2020;395(10223):496.].
2. Li Y, Xia L. Coronavirus Disease 2019 (COVID-19): Role of Chest CT in Diagnosis and Management. AJR Am J Roentgenol 2020;214(6):1280–1286.
3. Bernheim A, Mei X, Huang M, et al. Chest CT Findings in Coronavirus Disease-19 (COVID-19): Relationship to Duration of Infection. Radiology 2020;295(3):200463.
4. Bai HX, Hsieh B, Xiong Z, et al. Performance of radiologists in differentiating COVID-19 from viral pneumonia on chest CT. Radiology 2020. 10.1148/radiol.2020200823. Published online March 10, 2020.
5. Zhao W, Zhong Z, Xie X, Yu Q, Liu J. Relation Between Chest CT Findings and Clinical Conditions of Coronavirus Disease (COVID-19) Pneumonia: A Multicenter Study. AJR Am J Roentgenol 2020;214(5):1072–1077.
6. Chung M, Bernheim A, Mei X, et al. CT Imaging Features of 2019 Novel Coronavirus (2019-nCoV). Radiology 2020;295(1):202–207.
7. Salehi S, Abedi A, Balakrishnan S, Gholamrezanezhad A. Coronavirus Disease 2019 (COVID-19): A Systematic Review of Imaging Findings in 919 Patients. AJR Am J Roentgenol 2020. 10.2214/AJR.20.23034. Published online March 14, 2020.
8. Ellis SJ, Cleverley JR, Müller NL. Drug-induced lung disease: high-resolution CT findings. AJR Am J Roentgenol 2000;175(4):1019–1024.
9. Wang D, Hu B, Hu C, et al. Clinical Characteristics of 138 Hospitalized Patients With 2019 Novel Coronavirus-Infected Pneumonia in Wuhan, China. JAMA 2020;323(11):1061.
10. Gattinoni L, Chiumello D, Caironi P, et al. COVID-19 pneumonia: different respiratory treatments for different phenotypes? Intensive Care Med 2020;46(6):1099–1102.
11. Gattinoni L, Coppola S, Cressoni M, Busana M, Rossi S, Chiumello D. COVID-19 Does Not Lead to a "Typical" Acute Respiratory Distress Syndrome. Am J Respir Crit Care Med 2020;201(10):1299–1300.
12. Klok FA, Couturaud F, Delcroix M, Humbert M. Diagnosis of chronic thromboembolic pulmonary hypertension after acute pulmonary embolism. Eur Respir J 2020. 10.1183/13993003.00189-2020. Published online March 17, 2020.
13. Fox S, Akmatbekov A, Harbert JL, Li G, Brown JQ, Vander Heide RS. Pulmonary and Cardiac Pathology in Covid-19: The First Autopsy Series from New Orleans. medRxiv 2020.
14. Cui S, Chen S, Li X, Liu S, Wang F. Prevalence of venous thromboembolism in patients with severe novel coronavirus pneumonia. J Thromb Haemost 2020;18(6):1421–1424.
15. Danzi GB, Loffi M, Galeazzi G, Gherbesi E. Acute pulmonary embolism and COVID-19 pneumonia: a random association? Eur Heart J 2020;41(19):1858.
16. Hanley B, Lucas SB, Youd E, Swift B, Osborn M. Autopsy in suspected COVID-19 cases. J Clin Pathol 2020;73(5):239–242.
17. Zhang Y, Xiao M, Zhang S, et al. Coagulopathy and Antiphospholipid Antibodies in Patients with Covid-19. N Engl J Med 2020;382(17):e38.
18. Solaimanzadeh I. Acetazolamide, Nifedipine and Phosphodiesterase Inhibitors: Rationale for Their Utilization as Adjunctive Countermeasures in the Treatment of Coronavirus Disease 2019 (COVID-19). Cureus 2020;12(3):e7343.
19. Lang M, Som A, Mendoza DP, et al. Hypoxaemia related to COVID-19: vascular and perfusion abnormalities on dual-energy CT. Lancet Infect Dis 2020. 10.1016/S1473-3099(20)30367-4. Published online April 30, 2020.
20. Simpson S, Kay FU, Abbara S, et al. Radiological Society of North America Expert Consensus Statement on Reporting Chest CT Findings Related to COVID-19. Endorsed by the Society of Thoracic Radiology, the American College of Radiology, and RSNA. J Thorac Imaging 2020. 10.1097/RTI.0000000000000524. Published online April 28, 2020.
21. van der Meer RW, Pattynama PM, van Strijen MJ, et al. Right ventricular dysfunction and pulmonary obstruction index at helical CT: prediction of clinical outcome during 3-month follow-up in patients with acute pulmonary embolism. Radiology 2005;235(3):798–803.
22. Dudzinski DM, Hariharan P, Parry BA, Chang Y, Kabrhel C. Assessment of Right Ventricular Strain by Computed Tomography Versus Echocardiography in Acute Pulmonary Embolism. Acad Emerg Med 2017;24(3):337–343.
23. Burger IA, Husmann L, Herzog BA, et al. Main pulmonary artery diameter from attenuation correction CT scans in cardiac SPECT accurately predicts pulmonary hypertension. J Nucl Cardiol 2011;18(4):634–641.
24. Truong QA, Massaro JM, Rogers IS, et al. Reference values for normal pulmonary artery dimensions by noncontrast cardiac computed tomography: the Framingham Heart Study. Circ Cardiovasc Imaging 2012;5(1):147–154.
25. Dunham-Snary KJ, Wu D, Sykes EA, et al. Hypoxic Pulmonary Vasoconstriction: From Molecular Mechanisms to Medicine. Chest 2017;151(1):181–192.
26. Donahoe M. Acute respiratory distress syndrome: A clinical review. Pulm Circ 2011;1(2):192–211.
27. Grosse C, Grosse A. CT findings in diseases associated with pulmonary hypertension: a current review. RadioGraphics 2010;30(7):1753–1777.
28. Alsaad KO, Hajeer AH, Al Balwi M, et al. Histopathology of Middle East respiratory syndrome coronovirus (MERS-CoV) infection - clinicopathological and ultrastructural study. Histopathology 2018;72(3):516–524.
29. Nicholls JM, Poon LL, Lee KC, et al. Lung pathology of fatal severe acute respiratory syndrome. Lancet 2003;361(9371):1773–1778.
30. Barton LM, Duval EJ, Stroberg E, Ghosh S, Mukhopadhyay S. COVID-19 Autopsies, Oklahoma, USA. Am J Clin Pathol 2020;153(6):725–733.
31. Tian S, Hu W, Niu L, Liu H, Xu H, Xiao SY. Pulmonary Pathology of Early-Phase 2019 Novel Coronavirus (COVID-19) Pneumonia in Two Patients With Lung Cancer. J Thorac Oncol 2020;15(5):700–704.
32. Voltersvik P, Aqrawi LA, Dudman S, et al. Pulmonary changes in Norwegian fatal cases of pandemic influenza H1N1 (2009) infection: a morphologic and molecular genetic study. Influenza Other Respir Viruses 2016;10(6):525–531.
33. Greene R, Lind S, Jantsch H, et al. Pulmonary vascular obstruction in severe ARDS: angiographic alterations after i.v. fibrinolytic therapy. AJR Am J Roentgenol 1987;148(3):501–508.
34. Ackermann M, Verleden SE, Kuehnel M, et al. Pulmonary Vascular Endothelialitis, Thrombosis, and Angiogenesis in Covid-19. N Engl J Med 2020. 10.1056/NEJMoa2015432. Published online May 21, 2020.
35. Marini JJ, Gattinoni L. Management of COVID-19 Respiratory Distress. JAMA 2020;323(22):2329.
36. Gattinoni L, Chiumello D, Rossi S. COVID-19 pneumonia: ARDS or not? Crit Care 2020;24(1):154.
37. Cao W, Li T. COVID-19: towards understanding of pathogenesis. Cell Res 2020;30(5):367–369.
38. Lang M, Som A, Mendoza DP, et al. Hypoxaemia related to COVID-19: vascular and perfusion abnormalities on dual-energy CT. Lancet Infect Dis 2020. 10.1016/S1473-3099(20)30367-4. Published online April 30, 2020.
39. Johnson TR. Dual-energy CT: general principles. AJR Am J Roentgenol 2012;199(5 Suppl):S3–S8.
40. Otrakji A, Digumarthy SR, Lo Gullo R, Flores EJ, Shepard JA, Kalra MK. Dual-Energy CT: Spectrum of Thoracic Abnormalities. RadioGraphics 2016;36(1):38–52.
41. Stern EJ, Müller NL, Swensen SJ, Hartman TE. CT mosaic pattern of lung attenuation: etiologies and terminology. J Thorac Imaging 1995;10(4):294–297.
42. Ridge CA, Bankier AA, Eisenberg RL. Mosaic attenuation. AJR Am J Roentgenol 2011;197(6):W970–W977.
43. Castañer E, Alguersuari A, Gallardo X, et al. When to suspect pulmonary vasculitis: radiologic and clinical clues. RadioGraphics 2010;30(1):33–53.
44. Kobayashi T, Koyama S, Kubo K, Fukushima M, Kusama S. Clinical features of patients with high-altitude pulmonary edema in Japan. Chest 1987;92(5):814–821.
45. Koul PA, Khan UH, Hussain T, et al. High altitude pulmonary edema among "Amarnath Yatris". Lung India 2013;30(3):193–198.
46. Maggiorini M. High altitude-induced pulmonary oedema. Cardiovasc Res 2006;72(1):41–50.
47. Hackett PH, Roach RC. High-altitude illness. N Engl J Med 2001;345(2):107–114.
48. Xie Y, Wang X, Yang P, Zhang S. COVID-19 Complicated by Acute Pulmonary Embolism. Radiol Cardiothorac Imaging 2020;2(2):e200067.
49. Grillet F, Behr J, Calame P, Aubry S, Delabrousse E. Acute Pulmonary Embolism Associated with COVID-19 Pneumonia Detected by Pulmonary CT Angiography. Radiology 2020. 10.1148/radiol.2020201544. Published online April 23, 2020.

50. Leonard-Lorant I, Delabranche X, Severac F, et al. Acute Pulmonary Embolism in COVID-19 Patients on CT Angiography and Relationship to D-Dimer Levels. Radiology 2020. 10.1148/radiol.2020201561. Published online April 23, 2020.
51. Violi F, Cangemi R, Calvieri C. Pneumonia, thrombosis and vascular disease. J Thromb Haemost 2014;12(9):1391–1400.
52. Obi AT, Tignanelli CJ, Jacobs BN, et al. Empirical systemic anticoagulation is associated with decreased venous thromboembolism in critically ill influenza A H1N1 acute respiratory distress syndrome patients. J Vasc Surg Venous Lymphat Disord 2019;7(3):317–324 [Published correction appears in J Vasc Surg Venous Lymphat Disord 2019;7(4):621.].
53. Bahloul M, Chaari A, Kallel H, et al. Pulmonary embolism in intensive care unit: Predictive factors, clinical manifestations and outcome. Ann Thorac Med 2010;5(2):97–103.
54. Luo W, Yu H, Guo J, et al. Clinical pathology of critical patient with novel coronavirus pneumonia (COVID-19): pulmonary fibrosis and vascular changes including microthrombosis formation. 2020.